Membrane lipid poly-unsaturation selectively affects ligand induced dopamine D2 receptor internalization

Silvia Sposini[1,2]*, Rim Baccouch[3]*, Mathias Lescuyer[4], Véronique De Smedt-Peyrusse[5], Joyce Heuninck[4], Thierry Durroux[4], Pierre Trifilieff[5], David Perrais[1#], Isabel Alves[3]

[1] IINS, CNRS UMR 5297, 146 rue Léo-Saignat, 33076 Bordeaux, France

[2] IRDB, Department of Metabolism, Digestion and Reproduction, Imperial College London, London, United Kingdom

[3] CBMN, CNRS UMR 5248, Allée Geoffroy St Hilaire, 33600 Pessac, France

[4] IGF, Université de Montpellier, CNRS, Inserm

[5] Université de Bordeaux, INRAE, Bordeaux INP, NutriNeuro, 33000, Bordeaux, France.

*equal contribution

[#]corresponding author: david.perrais@u-bordeaux.fr

Keywords

Endocytosis; poly-unsaturated fatty acid; G protein coupled receptor; β-arrestin; β-adrenergic receptor; TIRF microscopy

Abstract

The poly-unsaturation of membrane phospholipids is an important feature for the biophysical properties of membranes and membrane proteins. In particular, it regulates the function of some G protein-coupled receptors (GPCR), such as their binding to ligand and G proteins or their membrane diffusion. However, its effects on GPCR internalization and trafficking remain unknown. The brain is highly enriched in poly-unsaturated fatty acids (PUFAs) and their deficiency has been associated with several neuropsychiatric disorders. Importantly, the Dopamine D2 receptor (D2R), a class A GPCR, is consistently impacted in these disorders and represents the main target of most antipsychotics. Here we show that enrichment in two different PUFAs strongly impairs agonist-induced endocytosis of D2R in HEK293 cells, without affecting clathrin-mediated endocytosis. Strikingly, this effect seems to be specific to the D2R as it does not affect various other GPCRs. Using live cell TIRF imaging, we show that D2R clustering is not affected, but that recruitment of β-arrestin2, that occurs prior to receptor internalization, is strongly impaired and endocytic vesicle formation is slowed down. Finally, we show that mutation of key residues in intracellular loop 2 abolishes the sensitivity of D2R

endocytosis to PUFA enrichment. We conclude that D2R trafficking is uniquely dependent on membrane PUFAs, which could influence its role in the control of brain activity and behavior.

Introduction

Cell signaling events almost systematically involve a complex interplay between protein and membrane remodeling. In particular, lipids are key regulators of membrane protein structure, conformational flexibility and activity. For example, in reconstituted in vitro systems, the activity of many G protein coupled receptors (GPCRs), the largest family of membrane receptors, such as rhodopsin, the serotonin $5HT_{1A}$ receptor or the chemokine CCR5 receptor, is strongly influenced by the presence of cholesterol in the membrane (Calmet *et al*, 2020; Pucadyil & Chattopadhyay, 2004; Jastrzebska *et al*, 2011; Pontier *et al*, 2008). Moreover, the nature of phospholipid head groups (phosphatidylcholine or phosphatidylethanolamine) also affects the binding of agonists or antagonists to GPCRs and their activation such as for the β2 adrenergic receptor (β2AR) (Dawaliby *et al*, 2016). Finally, the nature of the phospholipid fatty acid chains may also affect GPCR activity. Indeed, poly-unsaturated fatty acids (PUFAs) are necessary for preserving the optimal conformation and activity of GPCRs like rhodopsin and adenosine A_{2A} receptors (Mitchell *et al*, 1992; Niu *et al*, 2004; Grossfield *et al*, 2006; Mizumura *et al*, 2020).

PUFAs are fatty acid species that contain two or more unsaturations in their carbon chain. The position of the first carbon possessing an unsaturation, counted from the methyl end, known as omega, defines the type of PUFA, e.g. ω3 for first unsaturation at the third carbon atom from the methyl end. In the brain, PUFAs accumulate during *in utero* development and constitute roughly 30 % of total brain fatty acids in adulthood. They can modulate membrane properties, signaling pathways, and cell metabolism (Bazinet & Layé, 2014). Deficits in brain PUFA accumulation have been linked to several psychiatric disorders including major depressive disorder, bipolar disorder or schizophrenia (Garland *et al*, 2007; Berger *et al*, 2006). In particular, lower levels of ω3-PUFAs in the brain of individuals suffering from psychiatric disorders have been described (McNamara *et al*, 2007b, 2007a, 2008) and some studies have reported a significant advantage of ω3-PUFAs dietary supplementation for reducing symptoms (Robinson *et al*, 2019; Grosso *et al*, 2014). However, the molecular mechanisms by which PUFAs participate in the etiology of psychiatric symptoms remain largely elusive.

A common neurobiological phenotype found across many psychiatric disorders is a dysfunction in dopamine transmission, in particular, the activity of the dopamine D2 receptor (D2R) (Whitton *et al*, 2015; Beaulieu & Gainetdinov, 2011). Interestingly, ω3-PUFA deficiency in animal models have revealed alterations of dopamine transmission (Chalon, 2006) and a particular vulnerability of D2R-expressing neurons to ω3-PUFAs deficiency (Ducrocq *et al*, 2020). Mechanistically, molecular dynamics simulations show that membrane PUFA levels modulate the membrane diffusion rate of the D2R (Guixà-González *et al*, 2016). Moreover, enrichment in PUFAs in HEK-293 cells alters D2R ligand binding and signaling (Jobin *et al*, 2023). Altogether, these findings suggest a direct link between membrane PUFAs and the activity of the D2R.

Because the signaling efficiency mediated by D2R is directly related to the overall number of responsive receptors at the cellular membrane, which is controlled by internalization and desensitization processes, membrane PUFA composition, by affecting membrane biophysical properties (Barelli & Antonny, 2016; Baccouch et al, 2023) or GPCR conformation, could affect its trafficking. Activation by agonists leads to D2R phosphorylation by G protein receptor kinase 2/3 (GRK 2/3) on serine and threonine residues in the second and third intracellular loops (ICL2/3)(Namkung *et al*, 2009). This phosphorylation triggers robust recruitment of the cytoplasmic protein β-arrestin2, which binds and targets the phosphorylated receptor by scaffolding it to clathrin-coated pits, leading to its internalization into endosomes after dynamin-dependent membrane scission (Kim *et al*, 2001; Lan *et al*, 2009; Skinbjerg *et al*, 2009; Paspalas *et al*, 2006). Furthermore, β-arrestins also function as scaffold proteins that interact with cytoplasmic proteins and link GPCRs to intracellular signaling pathways such as MAPK cascades (Gurevich & Gurevich, 2006; Jean-Alphonse & Sposini, 2021; Peterson *et al*, 2015).

Here we investigated the modulatory effect of membrane lipid poly-unsaturation on ligand-induced D2R internalization. D2R-expressing HEK-293 cells were treated with either the ω3-PUFA docosahexaenoic acid (DHA) or the ω6-PUFA docosapentaenoic acid (DPA) in order to increase membrane poly-unsaturation in a controlled manner. Using resonance energy transfer-based technique or confocal microscopy, we demonstrated that PUFA membrane enrichment strongly blunted ligand-induced internalization of D2R but did not affect the internalization of transferrin, a cargo of clathrin mediated endocytosis (CME) or 7 other class A GPCRs. In addition, we found using Total Internal Reflection fluorescence (TIRF) microscopy that ligand-induced clustering of D2R was preserved in PUFA-enriched cells but that β-arrestin2 membrane recruitment was impaired and endocytic vesicle formation was reduced in conditions

of PUFA enrichment. Finally, we show that the unique sensitivity of D2R to PUFAs depends on two membrane proximal serine residues located in ICL2 of D2R.

Results

Robust incorporation of exogenous fatty acids into cell membranes

To assess the potential effects of membrane PUFAs on D2R trafficking, we used the protocol developed in (Jobin *et al*, 2023) to enrich membrane phospholipids with selected fatty acids. We evaluated the consequences of enrichment with 2 PUFAs, namely DHA or DPA, and the saturated fatty acid behenic acid (BA), all displaying 22 carbons (Figure 1A), allowing the distinction between the effect of number and position of unsaturations *versus* carbon chain length. Incubation for 24 h with 30 µM of DHA or DPA significantly increased the contents of PUFAs in phospholipids, from 8.6 % in control (EtOH) to ~14 %, while incubation with 30 µM of BA did not affect it significantly (Figure 1B). Conversely, the content of saturated fatty acids in phospholipids did not change after DHA or DPA treatment, while it was increased in BA treated cells (Figure 1C). Incubation with either fatty acid (DHA, DPA or BA) increased its respective content in phospholipids by at least 3 fold, leaving the content of the other fatty acids unaffected (Figure 1D-F). This shows that these treatments alter the cellular phospholipid composition in a fatty acid specific and controlled manner.

Consequently, the ratio of total ω6 (such as DPA) and ω3 (such as DHA) PUFAs (ω6/ω3) was significantly changed for cells treated with DHA (3-fold lower, $p < 0.01$) or DPA (2.7-fold higher, $p < 0.0001$), but not for cells treated with BA (Figure 1G). Despite the significant incorporation of these exogenous fatty acids into membrane lipids, these treatments did not induce any cell toxicity (Figure 1H), nor affected the level of expression of transfected tagged D2R at the plasma membrane (Figure 1I).

Impact of PUFA enrichment on D2R internalization investigated by DERET assay

We assessed the effect of PUFA enrichment on the internalization of D2R induced by multiple ligands in a dose-response manner using a high-throughput fluorometric assay, diffusion-enhanced resonance energy transfer (DERET) between the long life time luminescence donor Lumi-4-terbium (measured at 620 nm) attached to SNAP tagged D2R (SNAP-D2R) and the extracellular fluorescence acceptor fluorescein (peak fluorescence 520 nm) (Levoye *et al*, 2015). As illustrated in Figure EV1A, agonist-induced SNAP-D2R internalization is detected as a loss of energy transfer, leading to an increased fluorescence Ratio (620/520). Application

of the endogenous D2R agonist dopamine (10 μM) indeed resulted in a strong increase in Ratio (620/520) over time which was reversed by addition of the D2R antagonist haloperidol (10 μM) or the partial agonist aripiprazole (100 μM) 45 minutes after dopamine application (Figure EV1B, C). These latter findings are likely to result from the blocking effects of haloperidol and aripiprazole on dopamine-induced D2R internalization and to the recycling of the internalized D2R population to the cell surface. Taken together, these results confirm that DERET assay is a suitable technique to monitor agonist-induced D2R internalization in real time.

We next investigated the impact of DHA, DPA or BA enrichment on agonist-induced D2R internalization. Importantly, these treatments did not affect the level of D2R surface expression, as measured by SNAP-Lumi4-Tb fluorescence intensity at 620 nm (donor fluorescence) (Figure 1I). However, enrichment with either PUFAs (DHA or DPA) strongly blunted D2R internalization induced by either dopamine (Dopa) or the synthetic agonist quinpirole (QPL, Figure 2A, B). This effect of PUFAs was observed for all tested agonist concentrations. Dose-response curves, taken after 30 min stimulation, revealed a significant reduction of the maximal response (E_{max}) for PUFA-enriched cells (Figures 2C-E). However, no significant difference in dopamine-induced internalization efficacy (EC_{50}) was observed under membrane PUFA enrichments, while EC_{50} for quinpirole was significantly higher when compared to control cells (Figure 2F). These results were confirmed with dose-response curves obtained at later time points following agonist application (Figure EV2). Conversely, treatment with BA did not affect D2R internalization induced by neither dopamine nor quinpirole (10 μM) (Figure 1G, H). Altogether, these data indicate that the decrease in D2R internalization observed in membrane PUFA enriched cells is not related to the increased amount of long chain fatty acids (C22) but rather to the increased levels of membrane poly-unsaturation, independently of the position of the first unsaturation.

PUFA levels selectively affect D2R internalization without affecting general endocytosis

To get insight on the cellular mechanisms underlying blunted D2R ligand-induced internalization under membrane PUFA enrichment, we analyzed the steps of receptor internalization following agonist binding: D2R clustering at endocytic pits, recruitment of β-arrestin2 and formation of endosomes (Figure EV3) (Tsao & von Zastrow, 2000; Sposini & Hanyaloglu, 2018). We first examined the formation of endosomes with confocal microscopy. Cells expressing FLAG-D2R, GRK2 and β-arrestin2 were labelled live with anti-FLAG antibody for 10 min, incubated with or without D2R agonists (dopamine or quinpirole) for 30

min and fixed. As shown in Figures 3A and C, in the absence of D2R agonists, FLAG staining was mostly restricted to the cell perimeter, suggesting that the D2R has little constitutive internalization in all conditions of PUFA treatment. Addition of dopamine for 30 min triggered the formation of punctuate structures corresponding to internalized receptors. However, in DHA and DPA treated cells, the number of puncta induced by dopamine was much smaller than in untreated cells (34.5 ± 6.12 % and 29.5 ± 6 % for DHA and DPA compared to EtOH, respectively, $p < 0.0001$) (Figure 3A, B). Similar results were obtained in cells treated with the selective D2R agonist quinpirole (61.8 ± 6.9 % of control for DHA and 48.5 ± 7.3 % DPA, respectively, $p < 0.0001$) (Figure 3C, D). These results further show that cell enrichment with either PUFAs dampens agonist-induced D2R internalization.

D2Rs are internalized through CME (Paspalas *et al*, 2006). We thus tested if PUFA treatment affected the internalization of transferrin, a prototypical CME cargo (Doherty & McMahon, 2009). Fluorescently-labeled transferrin (Tfn-A568) uptake was assessed by confocal microscopy in both control and PUFA-enriched cells, incubated for 5 min at 37 °C in presence of Tfn-A568. As shown if Figure 4A, B, treatment with either DHA or DPA did not affect the number of Tfn-Alexa568 puncta after internalization for 5 min (105 % and 106 % of control for DHA and DPA, respectively, $p > 0.05$). Taken together, these results support that the specific effect of both PUFAs on ligand-induced D2R internalization is not due to an alteration of CME.

To examine whether the effect of DHA or DPA treatment was specific for the D2R or rather a more general mechanism for class A GPCRs, we examined the internalization of β2 adrenergic receptor (β2AR) following agonist stimulation (Goodman *et al*, 1996; von Zastrow & Kobilka, 1994). As shown in Figure 4C, the FLAG-tagged β2AR was mostly localized at the cell surface in the absence of agonist and internalized after addition of the synthetic agonist isoproterenol (10 μM). In striking difference with the results obtained with the D2R, the number of puncta was similar in control and PUFA-enriched cells (107 % and 101 % of control for DHA and DPA, respectively, $p > 0.05$) (Figure 4D).

We used again the DERET assay to test the effect of DHA or DPA treatment on various class A receptors: the δ, μ and κ opioid receptors (coupled to $G_{i/o}$ proteins, like D2R) and D1R, vasopressin receptor 2 (V2R), as well a β1- and β2ARs (coupled to G_s proteins). Only D2R showed sensitivity to PUFA treatments (Figure 4E). Altogether, these results suggest that PUFA enrichment specifically affects D2R internalization.

Membrane PUFAs do not alter D2R clustering but reduce the recruitment of β-arrestin2 and D2R endocytosis

Upon agonist stimulation, β-arrestin2 (βarr2) is recruited from the cytoplasm to activated D2R (Beaulieu *et al*, 2005; Skinbjerg *et al*, 2009). Once recruited, βarr2 and class A GPCRs cluster at clathrin coated pits with varying degrees (Goodman *et al*, 1996; Eichel *et al*, 2018). Therefore, we investigated D2R clustering and β-arr2 recruitment in cells transfected with D2R tagged with superecliptic pHluorin (SEP), a GFP mutant which is not fluorescent at pH 5.5, GRK2 and βarr2-mCherry, and imaged live with TIRF microscopy, as this technique allows to specifically focus on events happening at the plasma membrane or in its close proximity (~100 nm). As shown in Figure 5A and Movies EV1-3, SEP-D2R signal in control and PUFA-enriched cells was initially homogenous on the plasma membrane, then clustered following quinpirole stimulation. We quantitatively assessed this accumulation by measuring the fluorescence intensity at SEP-D2R clusters. Fluorescence quickly increased immediately after agonist application to reach a peak within ~100 s and slowly decreased thereafter (Figure 5B). The peak of SEP-D2R fluorescence was not significantly different in PUFA-enriched cells compared to control (Figure 5C). βarr2-mCherry was also recruited to SEP-D2R clusters following agonist application (Figure 5D,F). However, treatment with DHA or DPA significantly decreased peak βarr2-mCherry fluorescence (Figure 5F-G). This suggests a blunted βarr2 recruitment at D2R clusters. Similar results were obtained with cells treated with dopamine (Figure EV4).

To address the direct effect of blunted βarr2 recruitment on endocytic vesicle formation, we tested SEP-D2R endocytosis directly with the pulsed pH (ppH) assay (Sposini *et al*, 2020). In the ppH assay, cells are perfused alternatively every 2 s with buffers at pH 7.4 and 5.5. At pH 5.5, SEP-D2Rs on the plasma membrane are not fluorescent, revealing forming endocytic vesicles (Figure 6A). Endocytic vesicles containing SEP-D2R were thus detected by the ppH assay in images at pH 5.5 at preexisting SEP-D2R clusters, visible at pH 7.4, as shown in an example event (Figure 6B). Following quinpirole application, SEP-D2R and βarr2-mCherry clusters formed (Figure 6C), like in cells without pH changes (see Figure 5A, E). Moreover, quinpirole application induced an increase in the number of endocytic events detected compared to basal, and quinpirole removal led to decrease of endocytic vesicle formation (Figure 6C middle, Figure 6D and Movie EV4). While PUFA treatments did not change the number of SEP-D2R clusters detected after quinpirole application (Figure 6E), it significantly decreased the frequency of endocytic events detected by the ppH protocol (Figure 6F). We then

determined the fluorescence of SEP-D2R at the time of vesicle detection. It was affected neither at pH 7.4, reflecting the number of receptors in clusters (Figure 6G), nor at pH 5.5, reflecting the number of receptors in endocytic vesicles (Figure 6H). Moreover, averages of fluorescent traces aligned on vesicle detection (time 0) revealed that the kinetics of endocytic events were not affected by PUFA treatments (Figure 6J, K). Finally, the fluorescence of βarr2-mCherry at SEP-D2R clusters was significantly decreased in both DHA and DPA treated cells indicating a decreased number of βarr2 molecules recruited (Figure 6I). Moreover, βarr2-mCherry fluorescence was maximal at the time of vesicle detection in all three conditions (Figure 6L).

Finally, we tested again with the ppH assay the specificity of PUFA enrichment on the endocytosis of the constitutive cargo for clathrin-mediated endocytosis, the transferrin receptor tagged with Lime (TfR-Lime) (Merrifield *et al*, 2005; Shen *et al*, 2023). Consistent with our previous results on Tfn-A568 uptake (Figure 4A, B), the frequency of endocytic events detected with TfR-Lime or their amplitude in cells incubated with DHA or DPA was not significantly different from control cells (Figure EV5). Similarly, we tested with the ppH assay the internalization of SEP-β2AR (Shen *et al*, 2014) and the recruitment of βarr2-mCherry after application of isoproterenol (100 nM) (Movie EV5). Consistent with the results on FLAG-β2AR internalization (Figure 4C, D), treatment with DHA or DPA did not affect the frequency nor the amplitude of endocytic events (Figure EV6A-D), or the degree of βarr2-mCherry recruitment to endocytic clusters of SEP-B2AR (Figure EV6E, F).

Mutation of Serines 147 and 148 abolishes the PUFA sensitivity of D2R internalization

What could mediate the sensitivity of D2R to PUFA levels? Molecular dynamics simulation of D2R in membranes enriched or not with DHA showed that the conformation of the ICL2 region was changed in these two conditions (Jobin *et al*, 2023). In membranes without DHA, ICL2 sticks out of the membrane into the cytoplasm, making serines 147 and 148 accessible to cytosolic proteins. On the other hand, in membranes enriched with DHA, ICL2 is buried into the plasma membrane, with these two serines interacting mostly with lipid phosphatidyl groups. We thus mutated these two serines into alanines and tested the internalization of the mutated receptor FLAG-D2R(S147,148A) with confocal imaging of receptors labelled with anti-FLAG antibody for 30 min with or without quinpirole. In control cells (treated with vehicle), D2R(S147,148A) internalized after quinpirole application as much as WT D2R (Figure 7A, B). However, unlike WT D2R, treatment with DHA or DPA did not affect the internalization of D2R(S147,148A) (Figure 7C). This lack of effect was confirmed with the DERET assay (Figure 7D). Moreover, live cell imaging of cells co-transfected with SEP-D2R(S147,148A) and βarr2-

mCherry with the ppH assay showed that, during quinpirole application, treatments with DHA or DPA did not affect the frequency of endocytic events (Figure 7E), the fluorescence of SEP-D2R(S147,148A) clusters pH 7.4 (Figure 7F) and the recruitment of βarr2-mCherry at receptor clusters (Figure 7G). We conclude that mutations of serines 147 and 148 into alanines abolish the sensitivity of D2R to PUFA levels in membranes.

Discussion

Cell surface internalization of GPCRs is a highly regulated and multi-step process in which key protein-protein interactions have been identified (Magalhaes *et al*, 2012; von Zastrow & Sorkin, 2021). However, little information is available regarding the impact of membrane lipid composition on this mechanism. In the present study, we show that membrane enrichment with either the ω3-PUFA DHA or the ω6-PUFA DPA significantly decreased D2R internalization induced by two agonists (dopamine and quinpirole) with three different techniques: DERET, confocal microscopy and TIRF microscopy together with the ppH assay. The high throughput DERET assay showed with dose-response curves that both agonists have comparable efficacy (E_{max}) and potency (EC_{50}) to induce D2R internalization. In accordance, these full agonists have the same ability to activate D2R signaling (Brust *et al*, 2015; Jobin *et al*, 2023). Interestingly, membrane enrichment with either the ω3-PUFA DHA or the ω6-PUFA DPA reduces ligand-induced D2R internalization by about half at all concentrations of agonists tested, without affecting its overall internalization kinetics. However, while both dopamine- and quinpirole-induced maximum internalization levels (E_{max}) are decreased, only the EC_{50} of quinpirole-induced internalization is increased. D2R, like other GPCRs, is known to adopt multiple active conformational states depending on the ligand present in its binding pocket (Gay *et al*, 2004; Fan *et al*, 2020; Im *et al*, 2020; Yin *et al*, 2020; Zhuang *et al*, 2021). The different effect that PUFAs have on either quinpirole- or dopamine-induced D2R internalization (this study) and signaling (Jobin *et al*, 2023) could thus be explained by polyunsaturated acyl chains acting only on particular agonist-induced conformational states of the receptor. Of note, such a mechanism seems to be independent of the nature of the polyunsaturated chain (ω3 vs. ω6) and rather related to the overall amount of membrane unsaturation.

The level of PUFAs in membrane phospholipids could impact membrane compartmentalisation in lipid nanodomains, notably the integrity and stability of lipid rafts (Wassall & Stillwell, 2008; Levental *et al*, 2016). However, lipids rafts have been proposed to be signalling platforms for many GPCRs, including the D1R (Tiu *et al*, 2020) or the β2AR (Agarwal *et al*, 2018; Pontier *et al*, 2008), that we found insensitive to membrane PUFAs in internalization assays. The fatty acid composition of membrane lipids could also affect the biophysical properties of the membrane. Indeed, we have recently shown that enrichment of HEK 293 cells in DPA, but not DHA, affects both the elasticity and fluidity of the plasma membrane (Baccouch *et al*, 2023). Similarly, incorporation of DHA in retinal pigment epithelial-1 (RPE-1) cells affects their membrane bending rigidity (Pinot *et al*, 2014). Molecular dynamics simulations and

biochemical measurements suggest that DHA-containing phospholipids adapt their conformation to membrane curvature *via* their higher flexibility and make the plasma membrane more amenable to deformation by decreasing its bending rigidity (Manni *et al*, 2018). Consequently, Tfn endocytosis was increased in RPE-1 cells (Pinot *et al*, 2014). Despite a similar level of PUFA enrichment in our protocol (Jobin *et al*, 2023; Baccouch *et al*, 2023; this study) and in (Pinot *et al*, 2014), we found that PUFA enrichment in HEK 293 cells affected neither Tfn and TfR internalization, nor of other class A GPCRs, including $G_{i/o}$ coupled (δ, μ and κ opioid receptors, like D2R) and G_s coupled (D1R, β1- and β2AR, V2R) receptors, arguing against a general effect of PUFA enrichment on endocytosis.

Previous molecular dynamics simulation studies on the D2R have demonstrated that PUFA-containing phospholipids establish about three times more contacts with the D2R than phospholipids with monounsaturated chains, leading to the formation of a corona around the receptor (Guixà-González *et al*, 2016; Jobin *et al*, 2023), as shown also for other class A GPCRs, such as rhodopsin (Soubias *et al*, 2006) and the adenosine A_{2A} receptor (Yang & Lyman, 2019). This preferential interaction could alter the conformation of the D2R in the plasma membrane. Importantly, these simulations have shown that in a membrane with phospholipids enriched in PUFAs (DHA or DPA), the ICL2 of D2R is partially buried in the membrane, especially serines 147 and 148, while it remains fully water accessible in membranes without DHA. The ICL2 of the D2R is rich in polar and charged residues (Figure EV7) that would remain exposed to solvent. The PUFA-enriched membrane being more fluid and flexible than the non-enriched one results in a more favourable environment for ICL2 membrane insertion, rendering the process energetically favourable. ICL2 has been shown to participate in D2R internalization, together with ICL3 (Cho *et al*, 2010). It is therefore likely that the burying of ICL2 in the plasma membrane under PUFA enrichment could decrease its interaction with endocytic machinery such as β-arrestin, GRK, or other proteins such as GIPC, a necessary step for GPCR trafficking (Grimes *et al*, 2023; Patel *et al*, 2024). In accordance, we show that PUFA enrichment decreases agonist-induced βarr2 recruitment to receptor clusters at the membrane, a main step for internalization of many GPCRs, including the D2R (Skinbjerg *et al*, 2009; Clayton *et al*, 2014; Del'guidice *et al*, 2011), even though D2R internalization is partially independent of β-arrestins (Patel *et al*, 2024).

Consistent with this model, we show that mutation of the two consecutive serine residues (Ser 147 and 148), which are located at the ICL2-TM4 junction, does not affect D2R internalization in control, non PUFA-enriched cells, but preserves D2R internalization as well as β-arrestin

recruitment in high PUFA conditions. Polar serine residues can establish hydrogen bonds with the phospholipid head groups facilitating its proximity with the membrane. Their replacement by alanines makes the ICL2 significantly more hydrophobic which could change its conformation and membrane embedding properties rendering the double mutant insensitive to PUFAs. Interestingly, the two consecutive serines in D2R ICL2 are quite unique among class A GPCRs, as shown by sequence alignment (Figure EV7 and Supplementary Table 1). None of the 7 tested receptors has it (D1R has two serines located at the junction TM3-ICL2). Among the 200 class A non-orphan/non-opsin GPCRs, only D3R, nociceptin receptor (OPRX), lysophospholipid receptor S1PR5 and melatonin receptor MTR1a have consecutive serines in this region, although with very different flanking sequences. Therefore, PUFA sensitivity for internalisation is potentially shared with very few other class A GPCRs which could be provided by this double serine signature.

In the brain, GPCR internalization following agonist application mediates specific signalling and receptor desensitization (Kotowski *et al*, 2011; Jensen *et al*, 2017; Jullié *et al*, 2022). Interestingly, in substantia nigra pars compacta dopaminergic neurons, which strongly express D2Rs, internalization of the receptors in brain slices following agonist application (dopamine or quinpirole) was shown to be very limited, whereas another GPCR, μ-opioid receptor, was shown to undergo substantial internalization following agonist application in the same neurons (Robinson *et al*, 2017). Moreover, the same study showed that D2R ectopically expressed in locus coeruleus neurons strongly internalize upon agonist stimulation (Robinson *et al*, 2017). Although a number of associated signalling and scaffold proteins could regulate D2R trafficking, the present study raises the possibility that such an effect could be in part due to different PUFA composition between neuronal subtypes.

In conclusion, our results point to a potential mechanism by which lower PUFA levels described in several psychiatric disorders could directly participate in the aetiology of the diseases. Moreover, because PUFA levels can be modified, notably by dietary intake, the observation that PUFAs can directly alter the functionality and activity of the D2R opens up promising avenues for enhancing the efficacy of traditional pharmacological treatments such as antipsychotics for which the D2R is a main target.

Materials and methods

Cell culture and transfection

HEK-293 cells (ECACC, #12022001) were grown in DMEM supplemented with 10% Fetal Calf Serum and 1% penicillin/streptomycin in a 5% CO_2 enriched atmosphere at 37°C. Cells were passed twice a week and used between passages 8 and 20. HEK-293 cells were transfected with Lipofectamine®2000 for transient expression of tagged GPCR, βarr2 and GRK2, or TfR, with parameters adapted for the experiment (see below). SNAP-tagged human GPCRs were purchased from Revvity. FLAG-β2AR was described previously (Sposini *et al*, 2017). SEP-D2R was obtained based on SEP-LHR (Lutenizing Hormone Receptor) and FLAG-D2R (short isoform) constructs described previously in (Sposini *et al*, 2017) and (Guo *et al*, 2008), respectively. SEP was subcloned from SEP-LHR using AgeI and ligated into FLAG-D2R, containing an AgeI restriction site in the FLAG sequence created by site-directed mutagenesis (QuikChange Mutagenesis kit, Agilent) using oligonucleotides detailed in Reagents and Tools table. TfR-Lime and βarr2-mCherry were described previously (Shen et al. 2023) and (Boularan *et al*, 2007) respectively. FLAG-, SEP- and SNAP-tagged D2R(S147,148A), were created by site-directed mutagenesis (QuikChange Mutagenesis kit, Agilent) using oligonucleotides detailed in Reagents and Tools table and using Flag-, SEP- or SNAP-D2R WT as template, respectively.

For diffusion-enhanced resonance energy transfer (DERET) assays, cells were transfected as follows. White polyornithine 96-well plates were coated with poly-L-lysine (PLL, 50 µl of 0.1 mg/ml) for 30 min at 37 °C, then washed twice with 100 µl sterile phosphate buffered saline solution (PBS). After the washing step, a transfection mixture (50 µl/well) composed of 0.5 µl of Lipofectamine®2000, 5 ng of each of the following plasmids (N-terminal SNAP tagged GPCR, GRK2 and βarr2) and 185 ng of an empty vector were prepared in Opti-MEM reduced serum medium. After 20 min incubation at room temperature, the DNA/lipofectamine mixture was added to each well and followed by 100 µl of HEK-293 cells at a density of 250,000 cells/ml. Cells were grown 24 hours at 37 °C before the addition of PUFAs for 24 h before the DERET measures.

For confocal and TIRF microscopy experiments, cells were seeded in a 6 well plate in order to reach approximately 70 % confluence on the day of the transfection. Cells were transfected with a mixture (0.5 ml/well) containing 5 µl of Lipofectamine®2000 and 150 ng of each of the

following DNA (the N-terminally FLAG-D2R WT, FLAG- D2R(S147,148A) or FLAG-β2AR, the GRK2 and the βarr2) diluted in Opti-MEM medium and added dropwise to each well. For TIRF microscopy, cells were transfected with either 150 ng of SEP-D2R, WT, SEP-D2R(S147,148A) or SEP-β2AR, βarr2-mCherry and GRK2. For experiments with TfR, only TfR-Lime was transfected into the cells. Transfected cells were grown for 24 h at 37°C before incubation with PUFAs for another 24 h.

Cell fatty acid treatment and analysis

Fatty acids were dissolved in absolute ethanol under nitrogen at 30 mM and stored in aliquots until use. Cells were incubated with the different fatty acids as in (Jobin *et al*, 2023). Specifically, aliquots of each fatty acid were diluted in complete DMEM for a final concentration of 30 µM with a final fraction of 0.1% ethanol (EtOH, vehicle for control cells) for 24 h. Following incubation, cells were rinsed with complete DMEM to remove excess of fatty acids.

In order to ascertain exogenous fatty acid incorporation (DHA, DPA, BA), whole cell fatty acid analysis was performed as in (Jobin *et al*, 2023). Briefly, control and fatty acid treated cells were randomly analyzed according to (Joffre *et al*, 2016). Total lipids were extracted according to the method developed by (Folch *et al*, 1957) and transmethylated using 7 % boron trifluoride in methanol following (Morrison & Smith, 1964) protocol. Fatty acid methyl esters were extracted and analyzed by gas chromatography-flame ionization detector (GC-FID, Hewlett Packard HP5890, Palo Alto, CA). Fatty acid methyl esters were identified by comparison with commercial and synthetic standards and data analysis were processed using the Galaxie software (Varian). The proportion of each fatty acid was expressed as a percentage of total fatty acids to allow the comparison of lipid composition in different cell culture conditions.

Cell viability assay

Cell viability was measured using Resazurin Fluorimetric Cell Viability Assay. One day after treatment, control (ethanol) and fatty acid enriched cells were washed gently twice with pre-warmed PBS, and then a mixture of resazurin and DMEM in a ratio 1:10 was added into each well. After 3 h incubation at 37 °C, cell viability was monitored by measuring fluorescence with λ_{ex} at 540 nm and λ_{em} at 590 nm in a Tecan infinite M1000 Pro reader. The fluorescent signal generated in each well is directly proportional to the number of living cells in the sample.

The percentage of survival of fatty acid treated cells was calculated relative to control (EtOH) treated cells.

DERET assay and data analysis

Internalization assay was performed in white 96-well culture cell plates, using HEK-293 cells transfected with SNAP-D2R, GRK2, βarr2 and incubated with fatty acids, as described above. Cell culture medium was removed 24 h after PUFA treatment and 100 nM of SNAP-Lumi4-Tb (the donor fluorophore) previously diluted in Tag-lite buffer was added (50 µl/well) and further incubated for 1h at 16 °C to prevent/minimize receptor internalization. Excess SNAP-Lumi4-Tb was removed by washing each well four times with 100 µl of Tag-lite labeling buffer.

Membrane expression levels of the receptor were determined by measuring the fluorescence intensity of D2R-SNAP-Lumi4-Tb at 620 nm. Internalization experiments were performed by incubating cells with Tag-lite labeling buffer, either alone or containing one of the D2R ligands (Dopamine, Quinpirole, Aripiprazole, Haloperidol) in the presence of fluorescein (fluorescence acceptor). Typically, in plates containing SNAP-Lumi4-Tb-labeled cells, 90 µl of 25 µM fluorescein was added followed by the addition of 10 µl of ligand to reach a final concentration in the well ranging from 10^{-14} to 10^{-4} M. Fluorescence measurements were performed in a Tecan Infinite M1000 Pro plate reader, at 37°C right after the treatment described above.

For the experiments assessing D2R internalization kinetics, cells were stimulated with 10 µM of ligand. For dose response experiments, signals emitted by the donor (Lumi4-Tb) at 620 nm and by the acceptor (fluorescein) at 520 nm were collected at the indicated time points using time-resolved settings for the donor (1500 µs delay, 1500 µs reading time) and acceptor (150 µs delay, 400 µs reading time). The fluorescence intensity ratio 620/520 (R) was obtained by dividing the donor fluorescence signal (measured at 620 nm) by the acceptor fluorescence signal (measured at 520 nm) at a chosen time.

Data are expressed as percent of maximal internalization [% of max. internalization (620/520 nm)] using the following equation: $[(R_t - R_{min})/ (R_{max} - R_{min})] \times 100$ where R_t corresponds to the ratio observed at a chosen time, R_{min} and R_{max} correspond, respectively, to the minimum and the maximum fluorescence ratios. Data expressed in dose-response curves were fitted using non-linear regression dose-response and the following equation: $Y=Bottom + X*(Top-Bottom) / (EC_{50} + X)$, where X and Y represent the ligand concentration (log scale) and the maximum internalization (in percentage) allowing to obtain both the maximal effect (Emax) and half maximal effective concentration (EC_{50}) values.

Confocal microscopy imaging and data analysis

24 h before confocal imaging, glass slides were placed in a 12-well plate and coated with PLL (250 µl of 0.1 mg/ml) for 30 min at 37 °C. After coating, HEK-293 cells transiently expressing the FLAG-D2R, GRK2 and βarr2 (or FLAG-β2AR, GRK2 and βarr2) were seeded in complete DMEM containing 30 µM of PUFA or 0.1 % of EtOH. Cells were kept at 37 °C, 5% CO_2 for 24 hours to allow PUFA incorporation into cells.

For fixed cell imaging, cells were incubated with M1 anti FLAG antibody (1:500) for 10 min at 37° C and then left untreated or stimulated with ligands (dopamine or quinpirole for D2R, isoproterenol for β2AR) at 10 µM for 30 min. Cells were then washed with PBS (pH 7.4 containing 0.9 mM of Ca^{2+}) and fixed with 4% (v/v) paraformaldehyde diluted in Ca^{2+} enriched PBS for 10 min at room temperature. Fixed cells were permeabilized with 0.2% (v/v) Triton-X for 10 min and incubated with Alexa Fluor-555 anti-mouse antibody (1:1000) for 30 min at room temperature in the dark. Cells were washed 3 times with PBS and the coverslips were mounted on glass slides using Fluoromount.

Images were acquired with a spinning-disk confocal microscope (Leica DMI 6000B) controlled with MetaMorph (Molecular Devices), equipped with an EMCCD evolve camera and 561 nm diode laser. Images were analyzed using MetaMorph software and Matlab 2018a (MathWorks). Z-stack of twelve images separated with a fixed step size of 0.5 µm were acquired with a 63×/1.4 NA oil immersion objective. The maximal projections of the z-stacks were used to quantify the internalized receptors. A mask was traced around each cell as well as a background region using MetaMorph. The cell mask was eroded of 3 pixels (360 nm) to exclude the plasma membrane region containing receptors on the plasma membrane. Generated clusters of internalized receptors (FLAG-D2R or FLAG-β2AR) were detected by wavelet segmentation using custom written Matlab programs. For each cell, the number of clusters per mask was computed using a homemade Matlab script. These numbers were normalized to 100 for the control condition (cells grown in absence of PUFAs and incubated with receptor agonists) for each of the 3 independent experiments performed.

Transferrin uptake assay

HEK-293 cells were seeded on PLL coated glass coverslips and incubated with PUFAs as described above. After 24 h, cells were serum starved in pre-warmed DMEM for 30 min and then incubated for 15 min in cold DMEM containing 10 µg/ml Alexa Fluor 568-conjugated transferrin (Tfn-A568). Cells were incubated 5 min at 37 °C, allowing Tfn-A568 internalization, and washed in cold DMEM then in cold glycine buffer (100 mM NaCl, 50 mM

glycine, pH 3) for 2 min to remove Tfn-A568 bound to non-internalized TfR (stripping). Stripped cells were then fixed as explained above and kept at 4 °C until imaging. Fixed cell imaging and cluster quantification were performed in the same manner as described above for the GPCRs.

TIRF microscopy imaging and data analysis

Cells transiently expressing SEP tagged D2R, GRK2 and βarr2-mCherry were plated on PLL coated glass coverslips, grown in complete DMEM and then enriched with PUFAs as described above. 48 h after transfection and 24 h after PUFA enrichment, live cells were washed 2 times with FluoroBrite™ and imaged for 10 min in the same medium. The indicated D2R agonist was added at time 120 s, for experiments shown in time-courses. Live TIRF imaging was performed at 37°C in a temperature-controlled chamber under constant flow on a motorized Olympus IX83 inverted microscope outfitted with TIRF illuminator (Ilas2, Gataca Systems) with fiber coupled Laser sources (Cobolt Lasers 06-DPL 473 nm, 100 mW and 06-MLD 561 nm, 50 mW). Images were obtained with an Olympus TIRF objective (150X, 1.45 NA, oil immersion). Dual channel live acquisition was performed using 2 EMCCD cameras (QuantEM Model 512SC, Princeton Instruments) controlled by Metamorph 7.10 software (Molecular Devices). The gain of the EMCCD cameras was kept constant at 600, binning at 1 × 1, readout speed 10 MHz. Time lapse image sequences were acquired for up to 20 minutes at 0.5 Hz with an exposure time of 100 ms. Images of fluorescent beads (Tetraspeck microspheres, 0.2 µm) were acquired in every experiment as described previously (Sposini *et al*, 2020). Micro bead images were used to determine the precise parameters required for alignment of the two cameras; these parameters were then applied to all the images acquired on that day.

To quantify SEP-D2R and βarr2-mCherry fluorescence at clusters, the 11 images taken 100-120 s after addition of agonist, which corresponds to full clustering of SEP-D2R (see Figure 5B), were averaged. Clusters were detected by wavelet segmentation using custom written Matlab program. The movies were corrected for XY drift. Fluorescence values measured in the cluster regions were computed. The fluorescence values of the 60 frames before agonist addition were averaged and subtracted. The regions determined for SEP-D2R were transferred to the βarr2-mCherry channel with correction as described in the previous paragraph to compute βarr2-mCherry fluorescence values.

Pulsed pH (ppH) protocol

Cells transfected (with either SEP-D2R, GRK2 and βarr2-mCherry; SEP-D2R(S147,148A), GRK2 and βarr2-mCherry; SEP-β2AR, GRK2 and βarr2-mCherry; TfR-Lime) and enriched in PUFAs as described in the paragraph above were perfused with HEPES buffered saline solution (HBS) at 37 °C. HBS contained, in mM: 135 NaCl, 5 KCl, 0.4 $MgCl_2$, 1.8 $CaCl_2$, 1 D-glucose and 20 HEPES, and was adjusted to pH 7.4 and osmolarity of the medium cells were growing in. MES buffered saline solution (MBS) was prepared similarly by replacing HEPES with MES and adjusting the pH to 5.5 using NaOH. All salts were from Sigma Aldrich. HBS and MBS were perfused locally around the recorded cell using a 2-way borosilicate glass pipette as described in (Sposini *et al*, 2020). Movies were acquired at 0.5 Hz for a total of 900 s (GPCR) or 300 s (TfR). For experiments with SEP-D2R or SEP-β2AR, cells were imaged for 120 s, then agonist was added in both HBS and MBS channels at a final concentration of 10 µM (quinpirole) or 100 nM (isoproterenol) for 600 s, then was washed out for the remaining 180 s. For experiments with TfR-Lime cells were imaged for 300 s.

Detection of endocytic events and their analyses were conducted using custom made Matlab scripts previously described (Jullié *et al*, 2014; Rosendale *et al*, 2017; Sposini *et al*, 2020), apart from kymographs which were obtained using ImageJ. Endocytic events were automatically detected, defined as sudden punctate fluorescence increase appearing in pH 5.5 images, visible for more than 3 frames (i.e. 8 seconds) and appeared at the same location as a pre-existing fluorescence cluster detectable in pH 7.4 images. Event frequency was expressed per cell surface area measured on the cell mask. Fluorescence quantification of events was performed as in (Sposini *et al*, 2020). In short, each value is calculated as the mean intensity in a 2-pixel (206 nm) radius circle centered on the detection to which the local background intensity is subtracted (the local background is taken as the 20th to 80th percentile of fluorescence in an annulus of 5 to 2 pixel outer and inner radii centered on the detection). The frame of maximum intensity is used as the reference (time 0) for aligning and averaging all traces. Before (resp. after) tracking of an object the fluorescence is measured at the location of the first (resp. last) frame with the object tracked. Two color alignment was performed using an image of beads (TetraSpeck microspheres, ThermoFisher) taken before the experiment.

Statistical analysis

Data are presented as mean ± SEM (standard error of the mean). Statistical significance was determined using GraphPad Prism 8.3.0 (GraphPad, La Jolla, CA, USA). Normally distributed data sets were analyzed using one-way ANOVA or two-way ANOVA followed by Dunnett's

or Sidak's post-test were used when comparing more than two groups or at least two groups under multiple conditions, respectively. Differences were considered significant at $p < 0.05$. See Table 2 for values of all statistical tests performed in this study.

Acknowledgements

The authors are grateful to Prof Jonathan Javitch for providing the FLAG-D2R construct, Prof Aylin Hanyaloglu for the FLAG-β2AR construct, Dr Philippe Marin for the GRK2 construct and Dr Stefano Marullo for the β-arrestin2-mCherry construct. Imaging experiments involving spinning disk confocal microscopy were carried out at the Bordeaux Imaging Center, a service unit of the CNRS-INSERM and Bordeaux University, member of the national infrastructure France BioImaging supported by the French National Research Agency (ANR-10-INBS-04). We thank Magali Mondin for help with confocal microscopy. Figures EV1A and EV3 were created with BioRender®. The work was supported by the Agence Nationale de la Recherche (polyFADO ANR-21-CE44-0019 to TD, PT, DP and IA; LocalEndoProbes ANR-14-CE16-0012 and DopamineHub ANR-19-CE16-0003-01 to DP; FrontoFat ANR-20-CE14-0020 to PT), the Fondation Recherche Medicale team grants to PT and DP, University of Bordeaux's IdEx "Investments for the future" program/GPR BRAIN_2030 to PT and DP. SS is supported by a Sir Henry Wellcome postdoctoral fellowship (218650/Z/19/Z). RB PhD fellowship was obtained from the French Ministère de l'Enseignement Supérieur et de la Recherche.

Author contributions

RB, SS, TD, PT, DP, IA designed the study. RB, SS, ML, VDP, JH, DP performed the experiments and analyses. TD, PT, DP, IA provided funding. RB, SS, PT, DP, IA wrote the initial versions of the manuscript. All authors edited the manuscript.

Conflict of interest

The authors declare no competing financial interests.

References

Agarwal SR, Gratwohl J, Cozad M, Yang P-C, Clancy CE & Harvey RD (2018) Compartmentalized cAMP Signaling Associated With Lipid Raft and Non-raft Membrane Domains in Adult Ventricular Myocytes. *Front Pharmacol* 9

Baccouch R, Shi Y, Vernay E, Mathelié-Guinlet M, Taib-Maamar N, Villette S, Feuillie C, Rascol E, Nuss P, Lecomte S, *et al* (2023) The impact of lipid polyunsaturation on the physical and mechanical properties of lipid membranes. *Biochimica et Biophysica Acta (BBA) - Biomembranes* 1865: 184084

Bazinet RP & Layé S (2014) Polyunsaturated fatty acids and their metabolites in brain function and disease. *Nat Rev Neurosci* 15: 771–785

Beaulieu J-M & Gainetdinov RR (2011) The physiology, signaling, and pharmacology of dopamine receptors. *Pharmacol Rev* 63: 182–217

Beaulieu J-M, Sotnikova TD, Marion S, Lefkowitz RJ, Gainetdinov RR & Caron MG (2005) An Akt/beta-arrestin 2/PP2A signaling complex mediates dopaminergic neurotransmission and behavior. *Cell* 122: 261–273

Berger GE, Smesny S & Amminger GP (2006) Bioactive lipids in schizophrenia. *Int Rev Psychiatry* 18: 85–98

Boularan C, Scott MGH, Bourougaa K, Bellal M, Esteve E, Thuret A, Benmerah A, Tramier M, Coppey-Moisan M, Labbé-Jullié C, *et al* (2007) beta-arrestin 2 oligomerization controls the Mdm2-dependent inhibition of p53. *Proc Natl Acad Sci U S A* 104: 18061–18066

Brust TF, Hayes MP, Roman DL & Watts VJ (2015) New functional activity of aripiprazole revealed: Robust antagonism of D2 dopamine receptor-stimulated Gβγ signaling. *Biochem Pharmacol* 93: 85–91

Calmet P, Cullin C, Cortès S, Vang M, Caudy N, Baccouch R, Dessolin J, Maamar NT, Lecomte S, Tillier B, *et al* (2020) Cholesterol impacts chemokine CCR5 receptor ligand-binding activity. *FEBS J* 287: 2367–2385

Chalon S (2006) Omega-3 fatty acids and monoamine neurotransmission. *Prostaglandins Leukot Essent Fatty Acids* 75: 259–269

Cho D, Zheng M, Min C, Ma L, Kurose H, Park JH & Kim K-M (2010) Agonist-Induced Endocytosis and Receptor Phosphorylation Mediate Resensitization of Dopamine D2 Receptors. *Molecular Endocrinology* 24: 574–586

Clayton CC, Donthamsetti P, Lambert NA, Javitch JA & Neve KA (2014) Mutation of three residues in the third intracellular loop of the dopamine D2 receptor creates an internalization-defective receptor. *J Biol Chem* 289: 33663–33675

Dawaliby R, Trubbia C, Delporte C, Masureel M, Van Antwerpen P, Kobilka BK & Govaerts C (2016) Allosteric regulation of G protein-coupled receptor activity by phospholipids. *Nat Chem Biol* 12: 35–39

Del'guidice T, Lemasson M & Beaulieu J-M (2011) Role of Beta-arrestin 2 downstream of dopamine receptors in the Basal Ganglia. *Front Neuroanat* 5: 58

Doherty GJ & McMahon HT (2009) Mechanisms of Endocytosis. *Annual Review of Biochemistry* 78: 857–902

Ducrocq F, Walle R, Contini A, Oummadi A, Caraballo B, van der Veldt S, Boyer M-L, Aby F, Tolentino-Cortez T, Helbling J-C, *et al* (2020) Causal Link between n-3 Polyunsaturated Fatty Acid Deficiency and Motivation Deficits. *Cell Metabolism* 31: 755-772.e7

Eichel K, Jullié D, Barsi-Rhyne B, Latorraca NR, Masureel M, Sibarita J-B, Dror RO & von Zastrow M (2018) Catalytic activation of β-arrestin by GPCRs. *Nature* 557: 381–386

Fan L, Tan L, Chen Z, Qi J, Nie F, Luo Z, Cheng J & Wang S (2020) Haloperidol bound D2 dopamine receptor structure inspired the discovery of subtype selective ligands. *Nat Commun* 11: 1074

Folch J, Lees M & Sloane Stanley GH (1957) A simple method for the isolation and purification of total lipides from animal tissues. *J Biol Chem* 226: 497–509

Garland MR, Hallahan B, McNamara M, Carney PA, Grimes H, Hibbeln JR, Harkin A & Conroy RM (2007) Lipids and essential fatty acids in patients presenting with self-harm. *Br J Psychiatry* 190: 112–117

Gay EA, Urban JD, Nichols DE, Oxford GS & Mailman RB (2004) Functional selectivity of D2 receptor ligands in a Chinese hamster ovary hD2L cell line: evidence for induction of ligand-specific receptor states. *Mol Pharmacol* 66: 97–105

Goodman OB, Krupnick JG, Santini F, Gurevich VV, Penn RB, Gagnon AW, Keen JH & Benovic JL (1996) Beta-arrestin acts as a clathrin adaptor in endocytosis of the beta2-adrenergic receptor. *Nature* 383: 447–450

Grimes J, Koszegi Z, Lanoiselée Y, Miljus T, O'Brien SL, Stepniewski TM, Medel-Lacruz B, Baidya M, Makarova M, Mistry R, *et al* (2023) Plasma membrane preassociation drives β-arrestin coupling to receptors and activation. *Cell* 186: 2238-2255.e20

Grossfield A, Feller SE & Pitman MC (2006) A role for direct interactions in the modulation of rhodopsin by omega-3 polyunsaturated lipids. *Proc Natl Acad Sci U S A* 103: 4888–4893

Grosso G, Pajak A, Marventano S, Castellano S, Galvano F, Bucolo C, Drago F & Caraci F (2014) Role of omega-3 fatty acids in the treatment of depressive disorders: a comprehensive meta-analysis of randomized clinical trials. *PLoS One* 9: e96905

Guixà-González R, Javanainen M, Gómez-Soler M, Cordobilla B, Domingo JC, Sanz F, Pastor M, Ciruela F, Martinez-Seara H & Selent J (2016) Membrane omega-3 fatty acids modulate the oligomerisation kinetics of adenosine A2A and dopamine D2 receptors. *Sci Rep* 6: 19839

Guo W, Urizar E, Kralikova M, Mobarec JC, Shi L, Filizola M & Javitch JA (2008) Dopamine D2 receptors form higher order oligomers at physiological expression levels. *EMBO J* 27: 2293–2304

Gurevich VV & Gurevich EV (2006) The structural basis of arrestin-mediated regulation of G-protein-coupled receptors. *Pharmacol Ther* 110: 465–502

Im D, Inoue A, Fujiwara T, Nakane T, Yamanaka Y, Uemura T, Mori C, Shiimura Y, Kimura KT, Asada H, *et al* (2020) Structure of the dopamine D2 receptor in complex with the antipsychotic drug spiperone. *Nat Commun* 11: 6442

Jastrzebska B, Debinski A, Filipek S & Palczewski K (2011) Role of membrane integrity on G protein-coupled receptors: Rhodopsin stability and function. *Prog Lipid Res* 50: 267–277

Jean-Alphonse FG & Sposini S (2021) Confocal and TIRF microscopy based approaches to visualize arrestin trafficking in living cells. *Methods Cell Biol* 166: 179–203

Jensen DD, Lieu T, Halls ML, Veldhuis NA, Imlach WL, Mai QN, Poole DP, Quach T, Aurelio L, Conner J, *et al* (2017) Neurokinin 1 receptor signaling in endosomes mediates sustained nociception and is a viable therapeutic target for prolonged pain relief. *Science Translational Medicine* 9: eaal3447

Jobin M-L, De Smedt-Peyrusse V, Ducrocq F, Baccouch R, Oummadi A, Pedersen MH, Medel-Lacruz B, Angelo M-F, Villette S, Van Delft P, *et al* (2023) Impact of membrane lipid polyunsaturation on dopamine D2 receptor ligand binding and signaling. *Mol Psychiatry* 28: 1960–1969

Joffre C, Grégoire S, De Smedt V, Acar N, Bretillon L, Nadjar A & Layé S (2016) Modulation of brain PUFA content in different experimental models of mice. *Prostaglandins, Leukotrienes and Essential Fatty Acids* 114: 1–10

Jullié D, Benitez C, Knight TA, Simic MS & von Zastrow M (2022) Endocytic trafficking determines cellular tolerance of presynaptic opioid signaling. *eLife* 11: e81298

Jullié D, Choquet D & Perrais D (2014) Recycling Endosomes Undergo Rapid Closure of a Fusion Pore on Exocytosis in Neuronal Dendrites. *Journal of Neuroscience* 34: 11106–11118

Kim KM, Valenzano KJ, Robinson SR, Yao WD, Barak LS & Caron MG (2001) Differential regulation of the dopamine D2 and D3 receptors by G protein-coupled receptor kinases and beta-arrestins. *J Biol Chem* 276: 37409–37414

Kotowski SJ, Hopf FW, Seif T, Bonci A & von Zastrow M (2011) Endocytosis Promotes Rapid Dopaminergic Signaling. *Neuron* 71: 278–290

Lan H, Liu Y, Bell MI, Gurevich VV & Neve KA (2009) A dopamine D2 receptor mutant capable of G protein-mediated signaling but deficient in arrestin binding. *Mol Pharmacol* 75: 113–123

Levental KR, Lorent JH, Lin X, Skinkle AD, Surma MA, Stockenbojer EA, Gorfe AA & Levental I (2016) Polyunsaturated Lipids Regulate Membrane Domain Stability by Tuning Membrane Order. *Biophysical Journal* 110: 1800–1810

Levoye A, Zwier JM, Jaracz-Ros A, Klipfel L, Cottet M, Maurel D, Bdioui S, Balabanian K, Prézeau L, Trinquet E, *et al* (2015) A broad G protein-coupled receptor internalization assay that combines SNAP-tag labeling, diffusion-enhanced resonance energy transfer, and a highly emissive terbium cryptate. *Frontiers in Endocrinology* 6

Magalhaes AC, Dunn H & Ferguson SS (2012) Regulation of GPCR activity, trafficking and localization by GPCR-interacting proteins. *British Journal of Pharmacology* 165: 1717–1736

Manni MM, Tiberti ML, Pagnotta S, Barelli H, Gautier R & Antonny B (2018) Acyl chain asymmetry and polyunsaturation of brain phospholipids facilitate membrane vesiculation without leakage. *eLife* 7: e34394

McNamara RK, Hahn C-G, Jandacek R, Rider T, Tso P, Stanford KE & Richtand NM (2007a) Selective deficits in the omega-3 fatty acid docosahexaenoic acid in the postmortem orbitofrontal cortex of patients with major depressive disorder. *Biol Psychiatry* 62: 17–24

McNamara RK, Jandacek R, Rider T, Tso P, Hahn C-G, Richtand NM & Stanford KE (2007b) Abnormalities in the fatty acid composition of the postmortem orbitofrontal cortex of schizophrenic patients: gender differences and partial normalization with antipsychotic medications. *Schizophr Res* 91: 37–50

McNamara RK, Jandacek R, Rider T, Tso P, Stanford KE, Hahn C-G & Richtand NM (2008) Deficits in docosahexaenoic acid and associated elevations in the metabolism of arachidonic acid and saturated fatty acids in the postmortem orbitofrontal cortex of patients with bipolar disorder. *Psychiatry Res* 160: 285–299

Merrifield CJ, Perrais D & Zenisek D (2005) Coupling between Clathrin-Coated-Pit Invagination, Cortactin Recruitment, and Membrane Scission Observed in Live Cells. *Cell* 121: 593–606

Mitchell DC, Straume M & Litman BJ (1992) Role of sn-1-saturated,sn-2-polyunsaturated phospholipids in control of membrane receptor conformational equilibrium: effects of cholesterol and acyl chain unsaturation on the metarhodopsin I in equilibrium with metarhodopsin II equilibrium. *Biochemistry* 31: 662–670

Mizumura T, Kondo K, Kurita M, Kofuku Y, Natsume M, Imai S, Shiraishi Y, Ueda T & Shimada I (2020) Activation of adenosine A2A receptor by lipids from docosahexaenoic acid revealed by NMR. *Sci Adv* 6: eaay8544

Morrison WR & Smith LM (1964) PREPARATION OF FATTY ACID METHYL ESTERS AND DIMETHYLACETALS FROM LIPIDS WITH BORON FLUORIDE--METHANOL. *J Lipid Res* 5: 600–608

Namkung Y, Dipace C, Javitch JA & Sibley DR (2009) G Protein-coupled Receptor Kinase-mediated Phosphorylation Regulates Post-endocytic Trafficking of the D2 Dopamine Receptor *. *Journal of Biological Chemistry* 284: 15038–15051

Niu S-L, Mitchell DC, Lim S-Y, Wen Z-M, Kim H-Y, Salem N & Litman BJ (2004) Reduced G protein-coupled signaling efficiency in retinal rod outer segments in response to n-3 fatty acid deficiency. *J Biol Chem* 279: 31098–31104

Paspalas CD, Rakic P & Goldman-Rakic PS (2006) Internalization of D2 dopamine receptors is clathrin-dependent and select to dendro-axonic appositions in primate prefrontal cortex. *Eur J Neurosci* 24: 1395–1403

Patel NM, Ripoll L, Peach CJ, Ma N, Blythe EE, Vaidehi N, Bunnett NW, von Zastrow M & Sivaramakrishnan S (2024) Myosin VI drives arrestin-independent internalization and signaling of GPCRs. *Nat Commun* 15: 10636

Peterson SM, Pack TF, Wilkins AD, Urs NM, Urban DJ, Bass CE, Lichtarge O & Caron MG (2015) Elucidation of G-protein and β-arrestin functional selectivity at the dopamine D2 receptor. *Proceedings of the National Academy of Sciences* 112: 7097–7102

Pinot M, Vanni S, Pagnotta S, Lacas-Gervais S, Payet L-A, Ferreira T, Gautier R, Goud B, Antonny B & Barelli H (2014) Polyunsaturated phospholipids facilitate membrane deformation and fission by endocytic proteins. *Science* 345: 693–697

Pontier SM, Percherancier Y, Galandrin S, Breit A, Galés C & Bouvier M (2008) Cholesterol-dependent separation of the beta2-adrenergic receptor from its partners determines signaling efficacy: insight into nanoscale organization of signal transduction. *J Biol Chem* 283: 24659–24672

Pucadyil TJ & Chattopadhyay A (2004) Cholesterol modulates ligand binding and G-protein coupling to serotonin 1A receptors from bovine hippocampus. 1663: 188–200

Robinson BG, Bunzow JR, Grimm JB, Lavis LD, Dudman JT, Brown J, Neve KA & Williams JT (2017) Desensitized D2 autoreceptors are resistant to trafficking. *Scientific Reports* 7: 4379

Robinson DG, Gallego JA, John M, Hanna LA, Zhang J-P, Birnbaum ML, Greenberg J, Naraine M, Peters BD, McNamara RK, *et al* (2019) A potential role for adjunctive omega-3 polyunsaturated fatty acids for depression and anxiety symptoms in recent onset psychosis: Results from a 16 week randomized placebo-controlled trial for participants concurrently treated with risperidone. *Schizophr Res* 204: 295–303

Rosendale M, Jullié D, Choquet D & Perrais D (2017) Spatial and Temporal Regulation of Receptor Endocytosis in Neuronal Dendrites Revealed by Imaging of Single Vesicle Formation. *Cell Reports* 18: 1840–1847

Shen Y, Rosendale M, Campbell RE & Perrais D (2014) pHuji, a pH-sensitive red fluorescent protein for imaging of exo- and endocytosis. *The Journal of Cell Biology* 207: 419–432

Shen Y, Wen Y, Sposini S, Vishwanath AA, Abdelfattah AS, Schreiter ER, Lemieux MJ, de Juan-Sanz J, Perrais D & Campbell RE (2023) Rational Engineering of an Improved Genetically Encoded pH Sensor Based on Superecliptic pHluorin. *ACS Sens* 8: 3014–3022

Skinbjerg M, Ariano MA, Thorsell A, Heilig M, Halldin C, Innis RB & Sibley DR (2009) Arrestin3 mediates D(2) dopamine receptor internalization. *Synapse* 63: 621–624

Soubias O, Teague WE & Gawrisch K (2006) Evidence for specificity in lipid-rhodopsin interactions. *J Biol Chem* 281: 33233–33241

Sposini S & Hanyaloglu AC (2018) Evolving View of Membrane Trafficking and Signaling Systems for G Protein-Coupled Receptors. *Prog Mol Subcell Biol* 57: 273–299

Sposini S, Jean-Alphonse FG, Ayoub MA, Oqua A, West C, Lavery S, Brosens JJ, Reiter E & Hanyaloglu AC (2017) Integration of GPCR Signaling and Sorting from Very Early Endosomes via Opposing APPL1 Mechanisms. *Cell Reports* 21: 2855–2867

Sposini S, Rosendale M, Claverie L, Van TNN, Jullié D & Perrais D (2020) Imaging endocytic vesicle formation at high spatial and temporal resolutions with the pulsed-pH protocol. *Nature Protocols* 15, pages: 3088–3104

Taylor MJ, Perrais D & Merrifield CJ (2011) A High Precision Survey of the Molecular Dynamics of Mammalian Clathrin-Mediated Endocytosis. *PLoS Biology* 9: e1000604

Tiu AC, Yang J, Asico LD, Konkalmatt P, Zheng X, Cuevas S, Wang X, Lee H, Mazhar M, Felder RA, *et al* (2020) Lipid rafts are required for effective renal D1 dopamine receptor function. *The FASEB Journal* 34: 6999–7017

Tsao P & von Zastrow M (2000) Downregulation of G protein-coupled receptors. *Curr Opin Neurobiol* 10: 365–369

Wassall SR & Stillwell W (2008) Docosahexaenoic acid domains: the ultimate non-raft membrane domain. *Chemistry and Physics of Lipids* 153: 57–63

Whitton AE, Treadway MT & Pizzagalli DA (2015) Reward processing dysfunction in major depression, bipolar disorder and schizophrenia. *Curr Opin Psychiatry* 28: 7–12

Yang L & Lyman E (2019) Local Enrichment of Unsaturated Chains around the A2A Adenosine Receptor. *Biochemistry* 58: 4096–4105

Yin J, Chen K-YM, Clark MJ, Hijazi M, Kumari P, Bai X, Sunahara RK, Barth P & Rosenbaum DM (2020) Structure of a D2 dopamine receptor–G-protein complex in a lipid membrane. *Nature* 584: 125–129

von Zastrow M & Kobilka BK (1994) Antagonist-dependent and -independent steps in the mechanism of adrenergic receptor internalization. *J Biol Chem* 269: 18448–18452

von Zastrow M & Sorkin A (2021) Mechanisms for Regulating and Organizing Receptor Signaling by Endocytosis. *Annu Rev Biochem* 90: 709–737

Zhuang Y, Xu P, Mao C, Wang L, Krumm B, Zhou XE, Huang S, Liu H, Cheng X, Huang X-P, *et al* (2021) Structural insights into the human D1 and D2 dopamine receptor signaling complexes. *Cell* 184: 931-942.e18

Figures

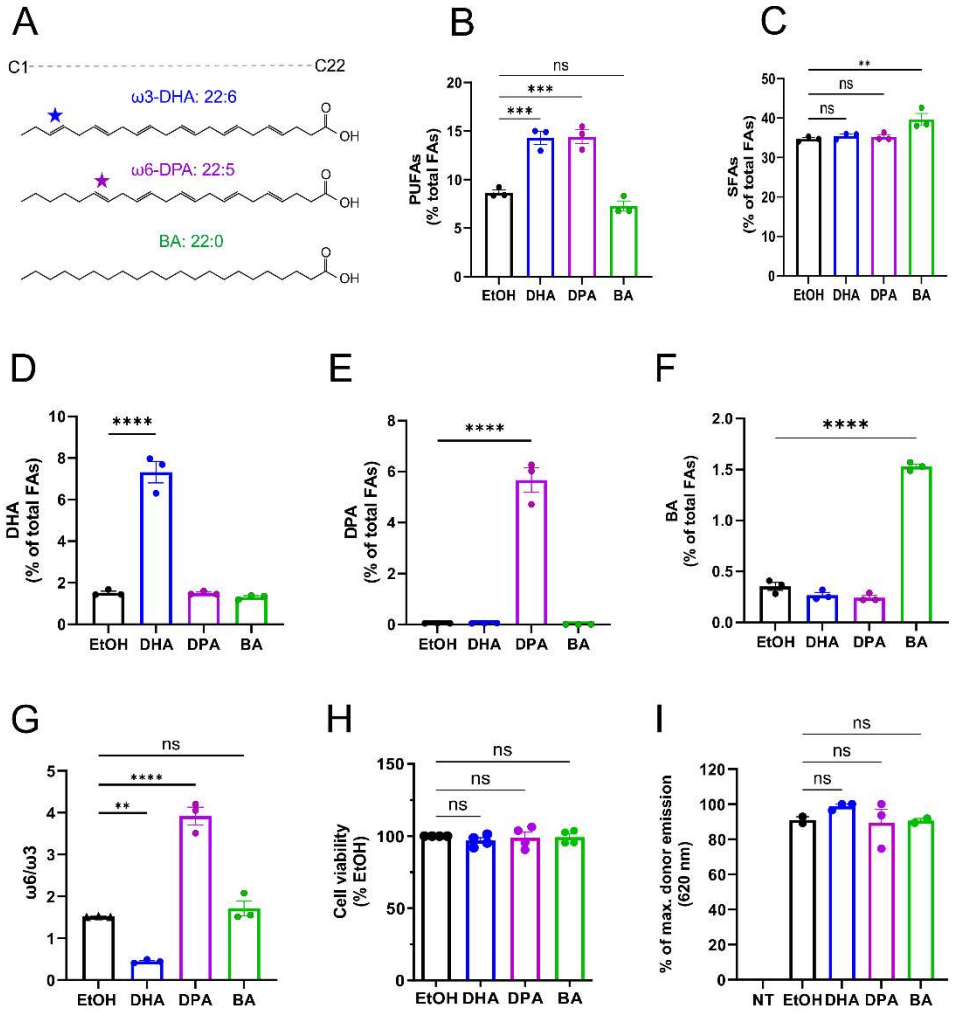

Figure 1: Phospholipid fatty acid enrichment in cells treated with exogenous fatty acids. A: Fatty acid structures: DHA (Docosahexaenoic acid), an ω3-PUFA with the formula $C_{22}H_{32}O_2$; DPA (Docosapentaenoic acid), an ω6-PUFA with the formula $C_{22}H_{34}O_2$. BA (behenic acid), a saturated fatty acid (SFA) with the formula $C_{22}H_{44}O_2$. **B, C:** Cellular amount of total PUFAs (B) and total SFAs (C), expressed as percentage of total phospholipid fatty acid (FA), measured in control (EtOH) and FAs (BA, DHA or DPA) treated cells (30 µM, 24 h). Control cells were treated in presence of 0.1 % of ethanol (EtOH, solvent used in BA and PUFAs solubilisation). **D-F:** Cellular amount of DHA (D), DPA (E) and BA (F), expressed as percentage of total phospholipid fatty acid, measured in control (EtOH) and cells treated with the corresponding fatty acid. **G:** Ratio of total ω6 and ω3 PUFAs (ω6/ω3) measured in control (EtOH) and fatty acid treated cells. **H:** Cell viability of control (EtOH) and FAs (BA, DHA or DPA) treated cells. **I:** D2R membrane expression levels measured by the SNAP-Lumi-4-Tb fluorescence intensity at 620 nm as for the DERET assays (see Figure 2) in non-transfected (NT) or cells co-expressing SNAP-D2R, β-arrestin2 and GRK2 treated with EtOH or FAs (BA, DHA, DPA). One-way ANOVA with Dunnett's multiple comparisons test of 3 independent experiments; ns $p \geq 0.05$, * $p<0.05$, ** $p<0.001$, *** $p<0.005$, **** $p<0.001$.

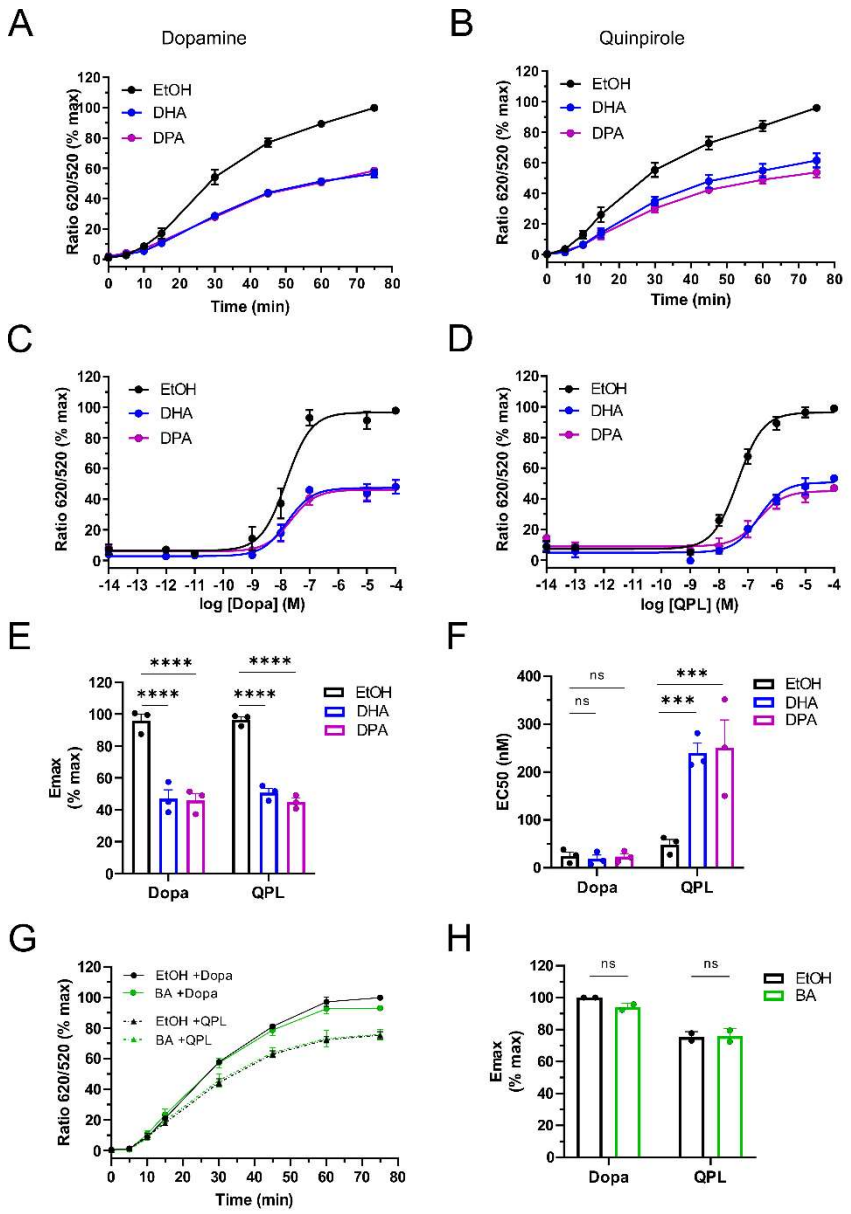

Figure 2: Impact of PUFA enrichment on D2R induced internalization assessed by DERET. A, **B**: Real-time internalization of SNAP tagged D2R upon Dopamine (A) or Quinpirole (B) stimulation (10 µM) of control (EtOH) and PUFA (DHA or DPA) enriched cells. Percentage of fluorescence ratio (ratio of the donor/acceptor fluorescence intensity; 620/520 nm) were plotted as a function of time. **C, D:** Dose–response curves of D2R agonist (Dopa, C; QPL, D) induced internalization following 30 min incubation at 37°C in presence of increasing concentrations of the indicated agonist. Data were fitted using non-linear regression dose–response and expressed as log [ligand] *versus* response for the 3 different conditions. **E, F:** Emax and EC_{50} values obtained from dose-response experiments of D2R internalization (C and D). **G:** Real-time internalization of SNAP tagged D2R expressed in control (EtOH) and BA-enriched cells upon stimulation with 10 µM of dopamine or quinpirole. **H**: Emax values measured in control and BA-enriched cells 30 min after dopamine or quinpirole stimulation. 3 independent experiments carried out in triplicates. Two-way ANOVA test with Sidak's multiple comparisons test; **** $p < 0.0001$, *** $p < 0.001$, ns $p \geq 0.05$.

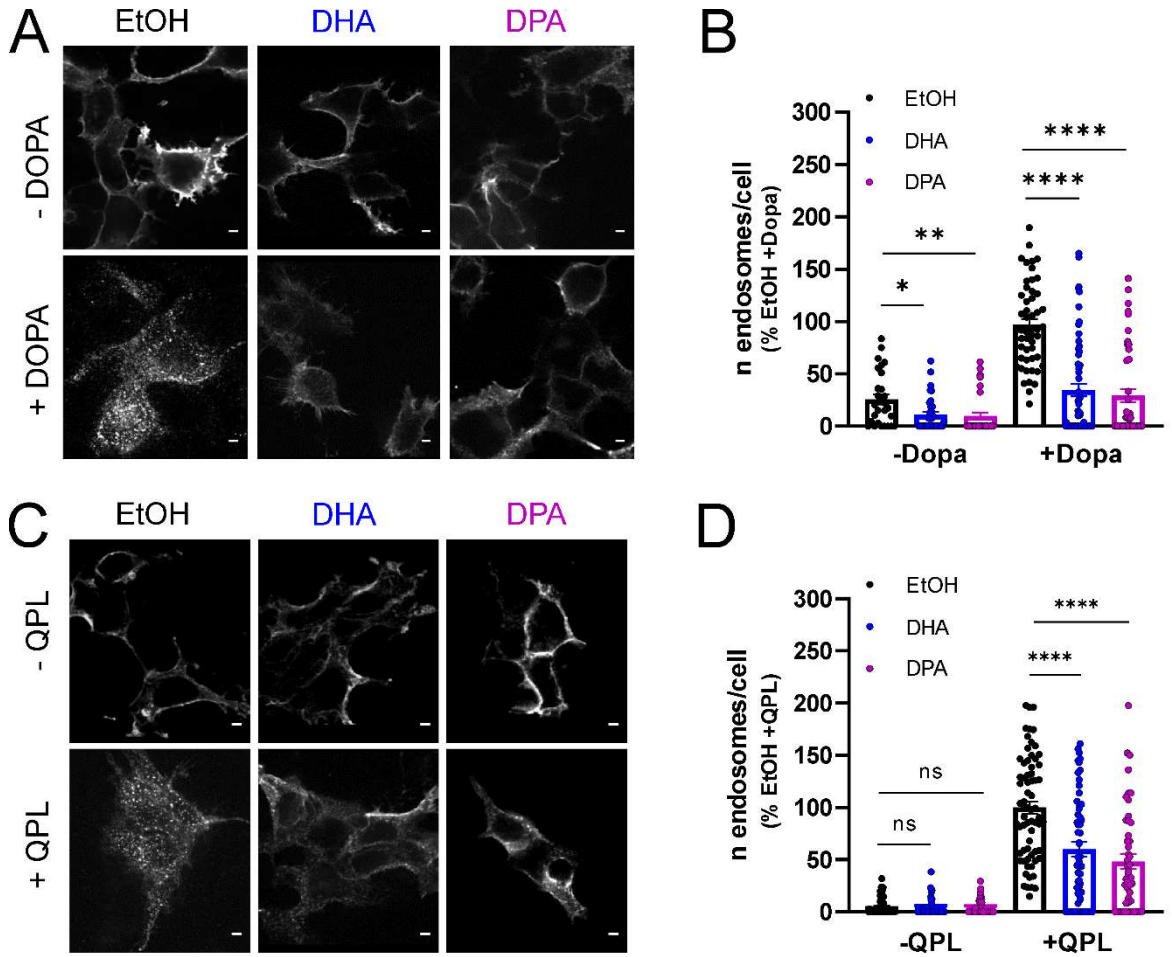

Figure 3: PUFA enrichment affects D2R internalization. **A, C:** Representative confocal microscopy images of control (EtOH) or PUFA-enriched (DHA or DPA) HEK-293 cells expressing FLAG-D2R, GRK2 and βarr2, before or after stimulation with either 10 µM of dopamine (Dopa) (A) or 10 µM of quinpirole (QPL) (C) for 30 min. Scale bar: 5 µm. **B, D:** Quantification of the number of D2R puncta (endosomes) generated before and after dopamine (Dopa) (B) or quinpirole (QPL) (D) stimulation in control (EtOH) and PUFA enriched cells. 68-71 cells per condition collected across 3 independent experiments. One-way ANOVA with Dunnett's multiple comparisons tests; * $p < 0.0001$, ** $p < 0.005$, **** $p < 0.0001$, ns $p \geq 0.05$.

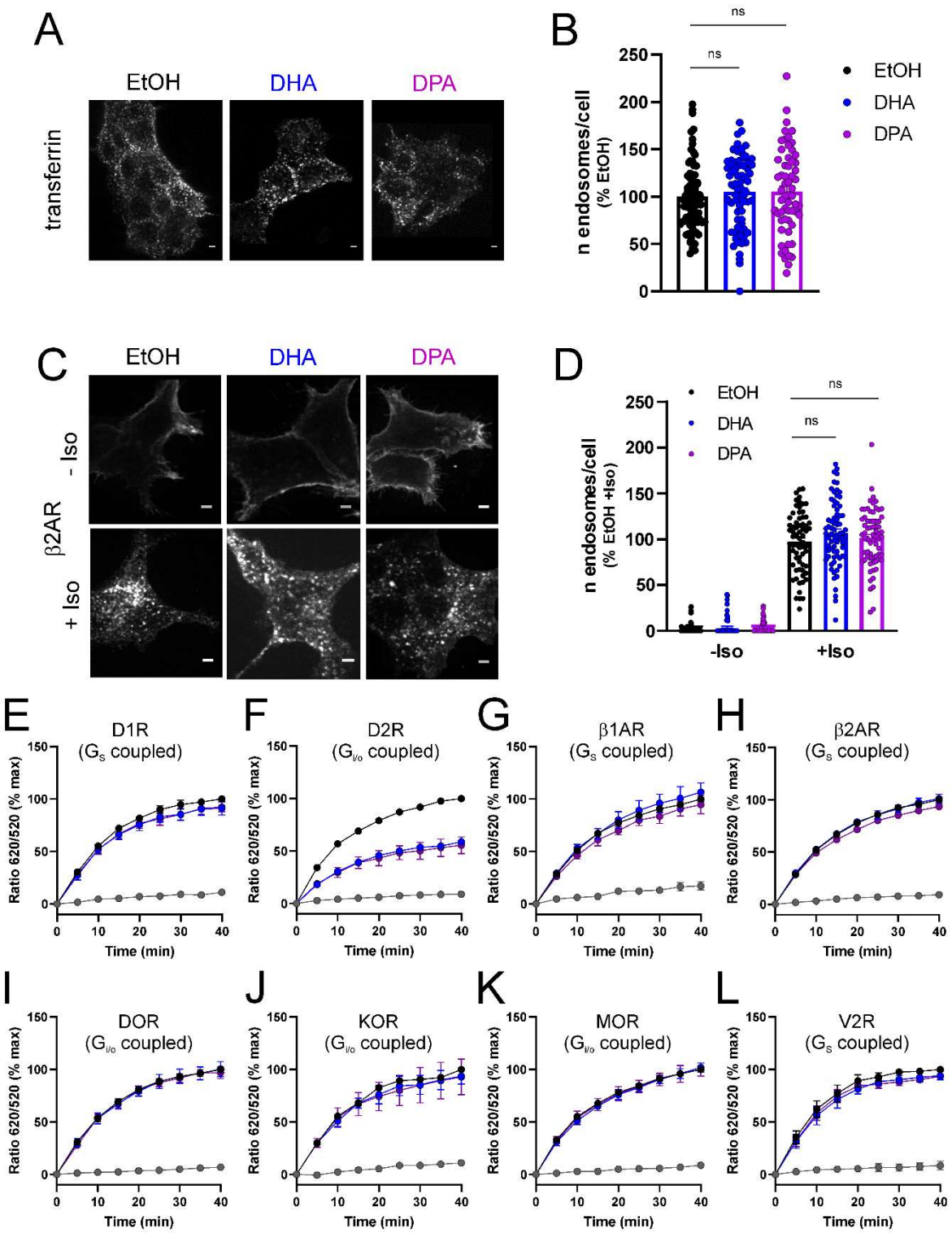

Figure 4: PUFAs do not alter internalization of transferrin or 7 class A GPCRs other than D2R. **A:** Representative confocal microscopy images of control (EtOH) or PUFA-enriched (DHA or DPA) HEK-293 cells incubated with fluorescently labeled transferrin for 5 min at 37 °C. Scale bar 5 µm. **B:** Quantification of the number of transferrin-labelled endosomes relative to control (EtOH); 64-74 cells per condition from 3 independent experiments. One-way ANOVA with Dunnett's multiple comparisons test: ns $p \geq 0.05$. **C:** Representative confocal microscopy images of control (EtOH) or PUFA-enriched (DHA or DPA) HEK-293 cells

expressing FLAG-β2AR, GRK2 and βarr2, before or after stimulation with 10 μM of isoproterenol (Iso) for 30 min. Scale bar 5 μm. **D:** Quantification of the number of β2AR puncta (endosomes) generated before and after Iso. 64-74 cells per condition collected across 3 independent experiments. One-way ANOVA with Dunnett's multiple comparisons test: ns $p \geq 0.05$. **E-L:** DERET assays for internalization of 8 class A GPCRs stimulated (black circles) or not (gray symbols) with selective agonists: SKF 81297 (1 μM) for SNAP-D1R (E); QPL (10 μM) for SNAP-D2R (F); Isoproterenol (10 μM) for SNAP-β1AR (G) and SNAP-β2AR (H); DPDPE (1 μM) for SNAP-DOR (I); U69593 (1 μM) for SNAP-KOR (J); DAMGO (1 μM) for SNAP-MOR (K); AVP (1 μM) for SNAP-V2R (L). Blue and magenta circles represent cells pretreated with DHA or DPA, respectively. The fluorescence ratio 620/520 is normalized to 100 for cells treated with vehicle (EtOH, black circles) at 40 min. Circles and error bars represent mean ± SEM for three independent experiments.

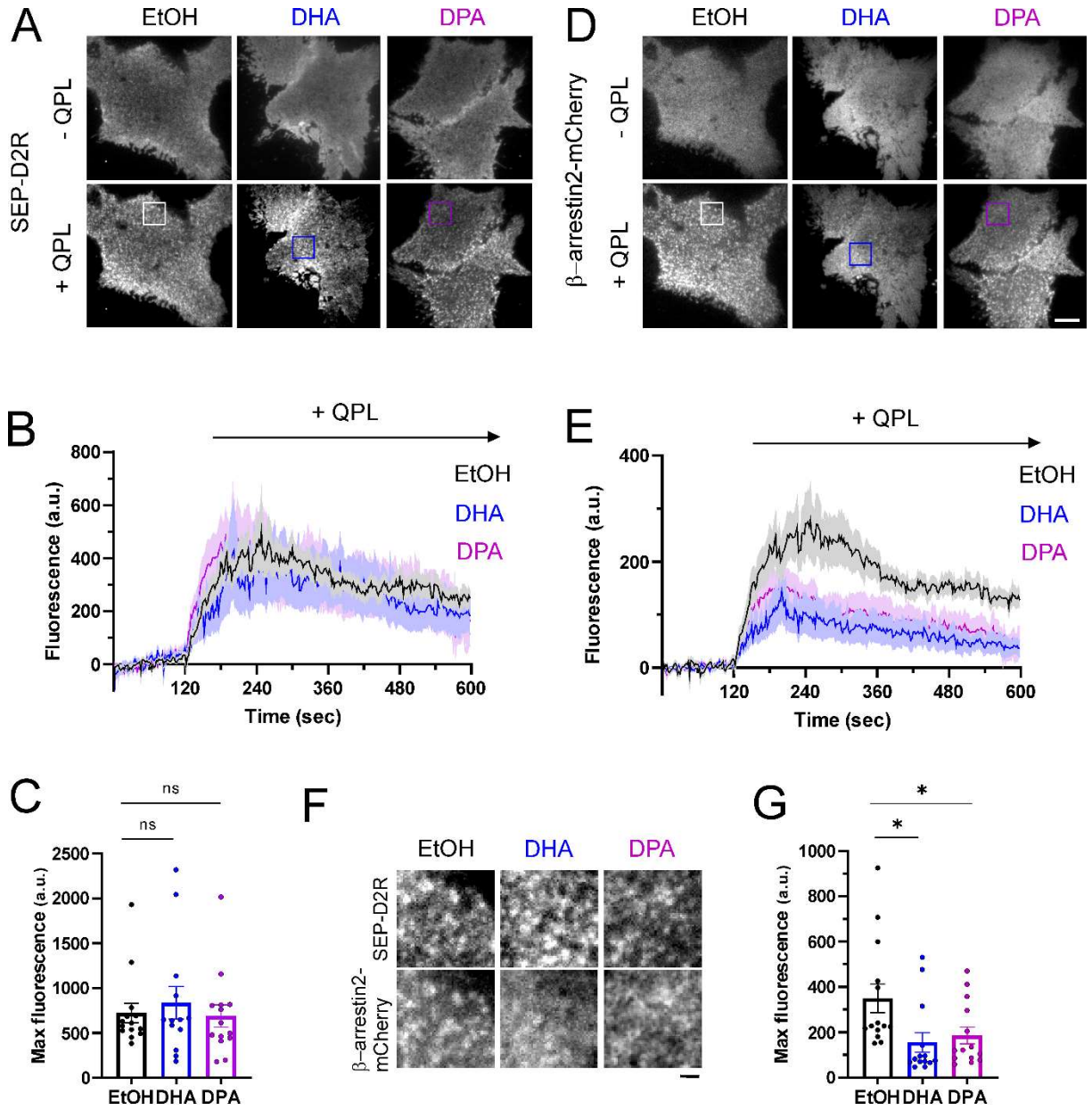

Figure 5: PUFA enrichment does not affect D2R clustering but reduces the recruitment of βarr2 after quinpirole addition. A, D: Representative TIRF microscopy images of HEK-293 cells co-expressing SEP-D2R, GRK2 and βarr2-mCherry in control (EtOH) or PUFA-enriched (DHA or DPA) cells, showing the pattern of expression at the plasma membrane for SEP-D2R (A) and βarr2-mCherry (D) before and after stimulation with 10 µM of quinpirole (QPL). Scale bar= 5 µm. See also Movies EV1-3. **B, E:** Mean Fluorescence intensity profiles of SEP-D2R (B) and βarr2-mCherry (E) obtained before and after quinpirole (QPL) addition (120 s after the start of the recording). Data represent average fluorescence values within each cluster minus average fluorescence before agonist addition. **C, G:** Maximum fluorescence intensities of SEP-D2R (C) and βarr2-mCherry (F) measured after QPL addition. Values represent maximum intensity fluorescence minus background fluorescence for 14 cells per condition collected across 3 independent experiments. One-way ANOVA test with Dunnett's multiple comparisons test; * $p < 0.05$, ns $p \geq 0.05$. **F:** Zoom-in images taken from panels in A and D, as shown by ROIs, depicting SEP-D2R and β-arrestin2-mCherry clusters after quinpirole addition. Scale bar= 1 µm.

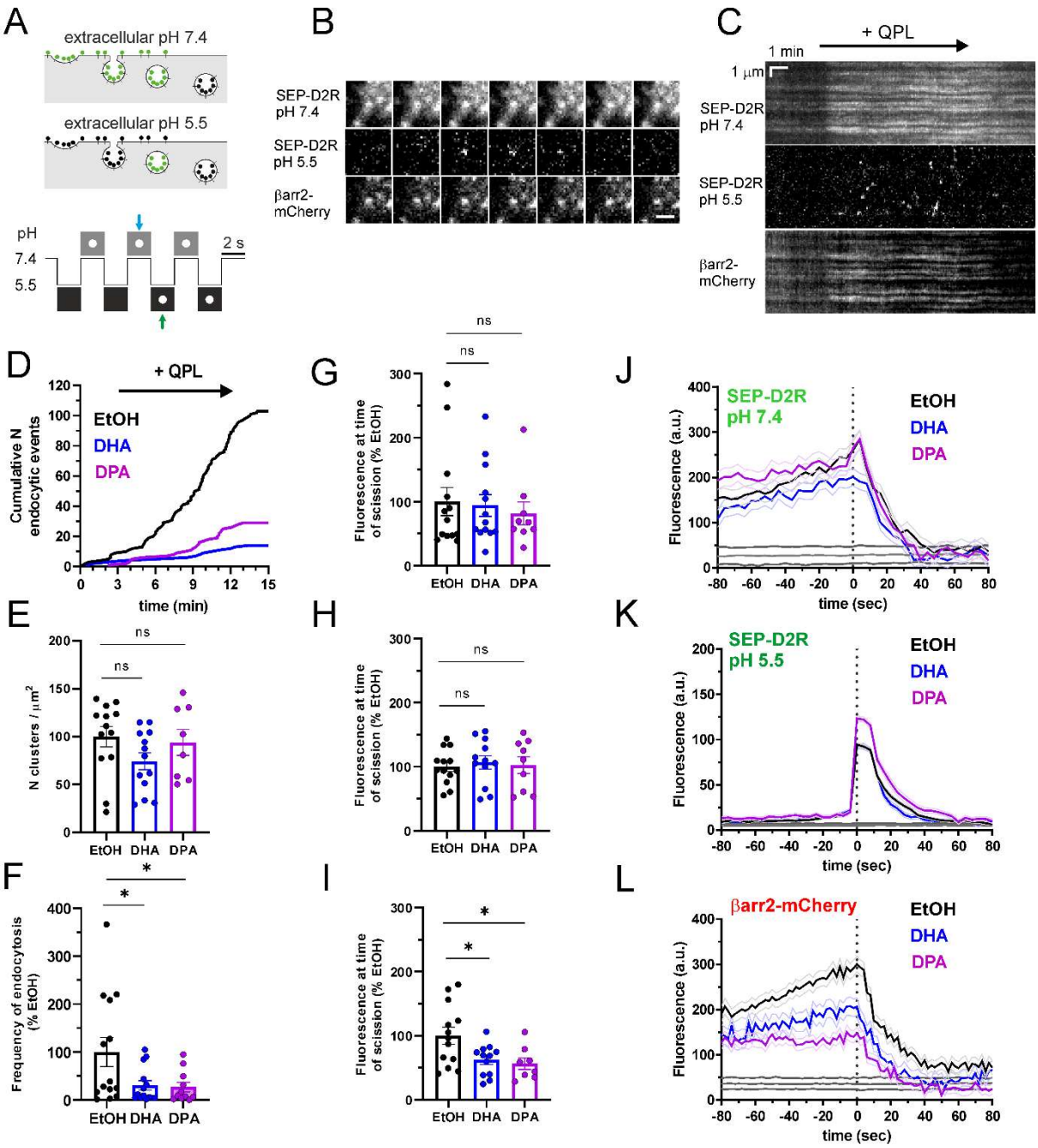

Figure 6: Reduction of endocytic vesicle formation and recruitment of βarr2 at nascent D2R endocytic vesicles in PUFA enriched cells. A: Top, experimental procedure: a cell expressing SEP-D2R is bathed in solutions alternating between pH 7.4 and 5.5. At pH 7.4, SEP-D2R on the plasma membrane and in non-acidic vesicles is visible (green lollipops). At pH 5.5, the surface receptors are not fluorescent (black lollipops), and the fluorescence from non-acidic CCVs is isolated. Bottom, principle of vesicle detection: a CCV formed at pH 7.4 (blue arrow) will be visible on the next image at pH 5.5 (green arrow). **B:** Example of a D2R cluster (top row), the corresponding endocytic event (middle row) and the associated β-arrestin2 cluster (bottom row) detected with the ppH protocol. Scale bar: 1 µm. **C:** Kymographs from a representative movie (Movie EV4) of a HEK-293 cells transfected with SEP-D2R, βarr2-mCherry and GRK2 and imaged live with the ppH protocol before (0-120 s), during (121-720 s) and after (701-900 s) application of 10 µM Quinpirole (QPL). **D:** Cumulative number of endocytic events detected with the ppH protocol in control (EtOH) or PUFA-enriched (DHA

or DPA) representative HEK-293 cell transfected and imaged as in C. **E:** Number of D2R clusters/cell detected during Quinpirole application in cells transfected as in C, treated with either EtOH, DHA or DPA and imaged live with the ppH protocol. One-way ANOVA with Dunnett's multiple comparisons test of 13, 13 and 8 cells treated with EtOH, DHA or DPA, respectively; ns $p \geq 0.05$ **F:** Number of endocytic events/min/μm^2 detected during Quinpirole application in cells transfected as in C, treated with either EtOH, DHA or DPA and imaged live with the ppH protocol. One-way ANOVA with Dunnett's multiple comparisons test of 14, 14 and 11 cells treated with EtOH, DHA or DPA, respectively; ** $p < 0.01$, * $p < 0.05$. **G-I:** Average fluorescence intensity of all events in a given cell, at the time of endocytic event detection, for SEP-D2R at pH7.4 (G), SEP-D2R at pH 5.5 (H) and β-arrestin2-mCherry at pH 5.5 (I) obtained from cells transfected and imaged as in C. One-way ANOVA test with Dunnett's multiple comparisons test for n= 13, 12 and 9 cells treated with EtOH, DHA and DPA, respectively; ** $p < 0.01$, * $p < 0.05$, ns $p \geq 0.05$. **J-L:** Average fluorescence over time of SEP-D2R at pH 7.4 (J), SEP-D2R at pH 5.5 (K) and β-arrestin2-mCherry at pH 5.5 (L), aligned to the time of vesicle scission (t = 0 s) obtained from terminal events (events for which the SEP-D2R cluster at pH 7.4 disappears within 80 s, defined as in (Taylor *et al*, 2011; Sposini *et al*, 2020) for the same cells used in G-I. Black lines represent 95% confidence intervals for randomized events to determine the level of enrichment at sites of scission. 424 terminal events from 13 cells (EtOH), 191 terminal events from 12 cells (DHA) and 254 terminal events from 9 cells (DPA).

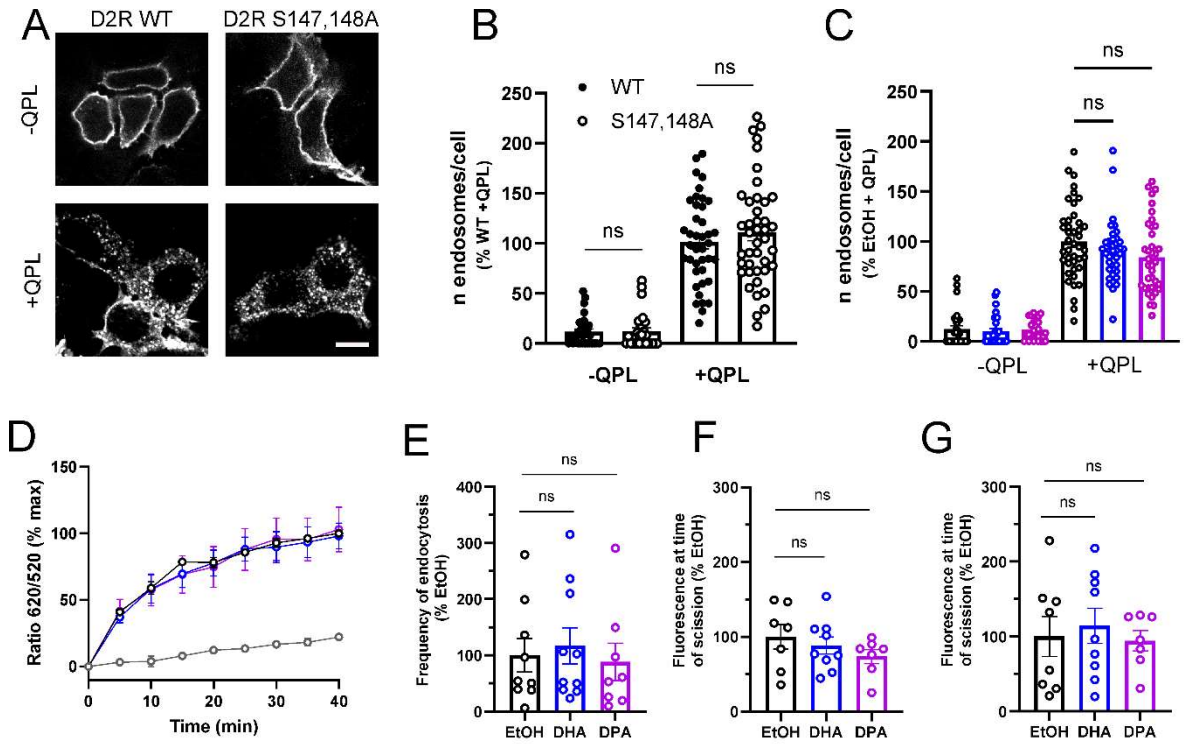

Figure 7: The internalization of the mutant D2R(S147,148A) is not modulated by DHA or DPA. A: Representative confocal microscopy images of control (EtOH) HEK-293 cells expressing FLAG tagged D2R or D2R(S147,148A), GRK2 and βarr2, before or after stimulation with 10 µM QPL for 30 min. Scale bar 5 µm. **B**: Quantification of the number of D2R puncta (endosomes) generated before and after QPL stimulation in untreated cells expressing FLAG tagged D2R WT or D2R(S147,148A). 40-42 cells per condition collected across 3 independent experiments. **C**: Quantification of the number of D2R(S147,148A) puncta (endosomes) generated before and after QPL stimulation in control (EtOH) and PUFA enriched cells. 25-42 cells per condition collected across 3 independent experiments; ns $p \geq 0.05$. **D**: DERET assay for internalization of SNAP- D2R(S147,148A) stimulated (black circles) or not (gray symbols) with QPL. **E:** Frequency of endocytic events detected during QPL application in cells transfected with SEP-D2R(S147,148A), βarr2-mCherry and GRK2, treated with either EtOH, DHA or DPA and imaged live with the ppH protocol (n = 9, 10 and 8, respectively, collected across 3 independent experiments; ns $p \geq 0.05$). **F, G:** Average fluorescence intensity of all endocytic events in a given cell, at the time of endocytic event detection, for SEP-D2R(S147,148A) at pH 7.4 (F), and β-arrestin2-mCherry (G) obtained from cells transfected and imaged as in E.

Table 1: Reagents and Tools Table

Reagent or tool	Source	Identifier
Antibodies		
Anti-FLAG M1 antibody	Sigma	F3040
Alexa Fluor 555 anti-mouse antibody	ThermoFisher Scientific	A31570
Buffers		
PBS		
DMEM	ThermoFisher Scientific	10564-011
FluoroBrite DMEM	ThermoFisher Scientific	A1896701
Tag-lite buffer	Revvity	LABMED
Chemicals, peptides and recombinant proteins		
Dopamine	Sigma	H8502
Quinpirole	Sigma	Q102
Haloperidol	Sigma	H1512
Aripiprazole	Sigma	SML0935
Docosahexaenoic acid, DHA	Sigma	D2534
Docosapentaenoic acid, DPA	Sigma	18566
Behenic acid, BA	Sigma	216941
Alexa Fluor 568-Tfn	ThermoFisher Scientific	T23365
Isoproterenol	Sigma	I6504
SKF81297	Tocris	1447
DPDPE	Sigma	5.08160
U69593	Sigma	U103
DAMGO	MedChemExpress	HY-P0210
AVP	Bachem	H-1780
TetraSpeck microspheres	ThermoFisher	T7280
Fluoromount-G	ThermoFisher	00-4958-02
Experimental models: cell lines		
HEK-293 cells	ECACC	12022001
Oligonucleotides		
SEP-D2R WT FW (5'-3')	tgttcgccgactacaagaccggtgatgacgccatggatcc	
SEP-D2R WT REV (5'-3')	ggatccatggcgtcatcaccggtcttgtagtcggcgaaca	
D2R(S147,148A) FW (5'-3')	tacaatacgcgctacgccgccaagcgccgggtcacc	
D2R(S147,148A) REV (5'-3')	ggtgacccggcgcttggcggcgtagcgcgtattgta	
Recombinant DNA		
SEP-D2R WT	This study	
FLAG-D2R WT	Prof. Jonathan Javitch, Columbia University	
SNAP-D2R WT	Revvity	
SEP-D2R(S147,148A)	This study	

FLAG- D2R(S147,148A)	This study	
SNAP- D2R(S147,148A)	This study	
TfR-Lime		(Shen *et al*, 2023)
FLAG-β2AR	Prof. Aylin Hanyaloglu, Imperial College London	
SEP-β2AR		(Jullie *et al*, 2014)
SNAP-β2AR	Revvity	
SNAP-β1AR	Revvity	
SNAP-D1R	Revvity	
SNAP-DOR	Revvity	
SNAP-KOR	Revvity	
SNAP-MOR	Revvity	
SNAP-V2R	Revvity	
βarrestin2-mCherry	Dr. Stefano Marullo, Institut Cochin	(Boularan *et al*, 2007)
βarrestin2	Revvity	
GRK2	Dr. Philippe Marin, Institut Genomique Fonctionnelle, Montpellier	
Software and algorithms		
Metamorph 7.10	https://www.moleculardevices.com/products/cellular-imaging-systems/acquisition-and-analysis-software/metamorph-microscopy	N/A
MATLAB 2018b	https://fr.mathworks.com	N/A
Custom MATLAB scripts	Scission_analysis (Sposini *et al*, 2020)	MATLAB Central File Exchange 72744-scission_analysis
ImageJ 1.53c	http://www.imagej.nih.gov/ij	N/A
Galaxie	Varian	
Kits		
QuickChange Mutagenesis kit	Agilent	200519